Life Sciences 235 (2019) 116800

Contents lists available at ScienceDirect

Life Sciences

journal homepage: www.elsevier.com/locate/lifescie

Trichostatin A inhibits skeletal muscle atrophy induced by cigarette smoke exposure in mice

Jingjing Ding[a,b], Fang Li[a,b], Yanfei Cong[a,b], Jianing Miao[a,b], Di Wu[a,b], Bo Liu[a,b], Lili Wang[a,b,*]

[a] *Medical Research Center of Shengjing Hospital, China Medical University, Shenyang 110004, China*
[b] *Key Laboratory of Research and Application of Animal Model for Environmental and Metabolic Diseases, Liaoning Province, China*

ARTICLE INFO

Keywords:
Cigarette smoking
Skeletal muscle
Atrophy
TSA
Pyroptosis

ABSTRACT

Aims: It is well known that cigarette smoke (CS) is the main risk factor for chronic obstructive pulmonary disease (COPD) accompanied by skeletal muscle atrophy. Histone deacetylases (HDACs) that remove acetyl groups from target proteins are necessary for the muscle atrophy associated with skeletal muscle disuse. However, the role of HDACs and trichostatin A (TSA), a HDAC inhibitor, in skeletal muscle atrophy caused by CS exposure remains poorly understood.
Main methods: Female mice were exposed to CS twice daily for 40 days and TSA injected intraperitoneally into CS-exposed mice on alternate days. Skeletal muscles were weighed and gastrocnemius (Gas) muscle histomorphology examined by hematoxylin and eosin staining. Histone deacetylases 1 and 2 (HDAC1/2), and markers of ubiquitin degradation, muscle differentiation, apoptosis, pyroptosis, and the cytoskeletal proteins were assessed by western blot and immunohistochemistry in Gas.
Keyfindings: CS exposure decreased body and skeletal muscle weights and triggered an increase in the percentage of fiber with centralized nuclei in Gas. HDAC1/2 proteins were upregulated in the Gas of mice exposed to CS, while TSA effectively inhibited HDAC1/2 protein levels and attenuated the loss of body weight and skeletal muscle wet weight induced by CS exposure. Markers for ubiquitin degradation, muscle differentiation, cytoskeletal proteins, apoptosis and pyroptosis were all upregulated following CS exposure and effectively restored by TSA.
Significance: TSA may inhibit skeletal muscle atrophy and histomorphological alterations induced by CS exposure by downregulating markers of ubiquitin degradation, muscle fiber differentiation, cytoskeletal proteins, apoptosis and pyroptosis via HDAC1/2 inhibition.

1. Introduction

Cigarette Smoking (CS) is prevalent worldwide and approximately 20% of the population smoke cigarette worldwide [1]. CS is probably the most significant source of toxic chemicals exposure to humans, which has been shown to be associated with adverse effects of skeletal muscle including skeletal muscle atrophy [2,3]. Several studies have examined the effect of CS on skeletal muscle atrophy. In chronic obstructive pulmonary disease (COPD), which is mainly caused by CS, muscle atrophy is one of the important comorbidities [4]. Steffl M et al. found that CS as an isolated factor may contribute to the development of sarcopenia [5]. However, the exact mechanisms involved in CS causing muscle atrophy are unknown.

Histone deacetylases (HDACs) modulate gene transcription and protein function by regulating the level of acetylation of histones and other proteins. HDACs also participate in the regulation of the activity of many transcription factors and large macromolecular complexes involved in a variety of cellular processes [6]. The specific knockdown of HDAC1 and HDAC2 (HDAC1/2) in skeletal muscle causes a proportion of mice pups to die during the perinatal period due to mitochondrial abnormalities and sarcomere degeneration [7]. HDACs, specifically HDAC1, remove acetyl groups from target proteins and are necessary for the muscle atrophy and contractile dysfunction associated with skeletal muscle disuse [8]. The upregulation of Forkhead box O (FOXO) transcription factors, one of the target proteins of HDAC1, is essential for skeletal muscle atrophy. HDAC1 promotes muscle atrophy by increasing the FOXO-dependent transcription of target genes involved in the ubiquitin proteasome pathway (tripartite motif 63 [*TRIM63*] and F-box protein 32 [*FBXO32*]), autophagy (microtubule associated protein 1 light chain 3 alpha [*LC3*]) and in the inhibition of protein synthesis

* Corresponding author at: Medical Research Center of Shengjing Hospital, No.7 Mulan Road, Benxi City, Liaoning Province, China.
E-mail address: llwang@cmu.edu.cn (L. Wang).

https://doi.org/10.1016/j.lfs.2019.116800
Received 4 June 2019; Received in revised form 21 August 2019; Accepted 27 August 2019
Available online 28 August 2019

(eukaryotic translation initiation factor 4E binding protein, [*4EBP*]) [8]. Trichostatin A (TSA), a HDAC inhibitor, prevents skeletal muscle atrophy that may be due to the regulation of the *TRIM63* gene [9]. Treatment with TSA ameliorates muscle atrophy and neuromuscular junction denervation, delays disease progression and increases survival in a mouse model of amyotrophic lateral sclerosis; it also improves body weight and survival in spinal muscular atrophy mice [10,11]. Moreover, TSA treatment in the early frog embryo induces selective inhibition of the transcriptional induction of the *myoD* gene and a severe reduction of subsequent muscle differentiation [12]. Based on the above studies, we hypothesized that HDACs may be involved in skeletal muscle abnormalities caused by CS exposure by regulating protein synthesis and degradation and muscle fiber differentiation.

In addition, the upregulation of the P2X purinergic receptor, a ligand-gated ion channel (P2RX7), and an ATP-gated ion channel need high levels of extracellular ATP in dystrophic muscle cells and induce a number of mechanisms, including apoptosis and pyroptosis [13–15]. Previous studies have found that apoptosis and pyroptosis were associated with the skeletal muscle atrophy observed in COPD [16–18]. Therefore, in this work we also explored whether P2RX7-mediated pyroptosis and apoptosis were involved in skeletal muscle damage caused by CS exposure.

The purpose of the current study was to investigate the mechanism of HDAC involvement in skeletal muscle atrophy caused by CS exposure and the therapeutic potential of TSA in this process.

2. Materials and methods

2.1. Animals

Female C57BL/6 mice(8 weeks old at the start of CS exposure) were supplied by the Animal Center of Shengjing Hospital at China Medical University. All animal experiments were conducted in accordance with the protocol approved by the Institutional Animal Care and Use Committee of the China Medical University (No. 2013PS06K). All mice were maintained on a standard 12-h light/dark cycle, free access to food and water and under controlled temperatures (25 ± 1 °C) and humidity (50 ± 10%).

2.2. CS exposure

The XiongShi brand of cigarettes (China Tobacco Zhejiang Industrial Co., LTD, Zhejiang, China), with each cigarette containing 0.7 mg of nicotine and 8 mg of tar, was used in this study. CS exposure, and TSA doses and methods were based on those used in our previous study [19]. After habituation for seven days, the mice were divided into three groups: room air exposure (Control), cigarette smoke exposure (CS) and cigarette smoke exposure + trichostatin A (CS + TSA; T1952-200UL; Sigma, St Louis, MI, USA), at least five mice in each group. Mice in the Control group were placed in a restrainer for 120 min, twice daily, and exposed to room air only for a duration of 40 days. Mice in the CS exposure group were exposed to CS in a whole-body exposure system for 120 min, twice daily, for duration of 40 days. TSA (0.6 mg/kg body weight on alternate days for 40 days) was injected intraperitoneally into the mice of the CS + TSA group. All mice were weighed every day. After CS exposure for 10, 20, 30 and 40 days, at least five mice in each group were euthanized and the gastrocnemius (Gas), tibialis anterior (TA) and triceps (Tri) muscles were collected for further studies. In this study, the target proteins, except autophagy-related proteins, were detected in the Gas of mice treated with CS for 40 days.

2.3. Hematoxylin and eosin staining

After 40 days of CS exposure, two each of Gas, TA and Tri muscles from each animal were harvested and weighed from at least five mice in each group. One Gas of each animal was promptly fixed in 4% paraformaldehyde for 24 h, then embedded with paraffin and cut into cross-sections (4 μm thick). After this, hematoxylin and eosin (HE) staining was performed. Another Gas of each animal was quickly frozen in liquid nitrogen for the subsequent detection of protein expression. Gas histomorphology was examined by a Nikon Ni upright microscope using bright field microscopy with 40× objective lenses and photographed using Nis-Elements software.

2.4. Western blot

Total proteins were extracted from Gas using RIPA buffer (Beyotime, Jiangsu, China) containing phenylmethylsulfonyl fluoride to inhibit proteases. Protein concentrations were measured using a BCA Protein Assay Kit (Thermo, Waltham, MA, USA). Samples with equal amounts of protein were separated by 12.5% sodium dodecyl sulfate–polyacrylamide gel electrophoresis (SDS–PAGE), and immunoblot analysis performed on polyvinylidene difluoride membranes (PVDF; Millipore Corporation, Burlington, MA, USA). Following blocking in 5% non-fat milk for 1 h at room temperature, the PVDF membranes were incubated with primary antibodies at 4 °C overnight and for another 1 h at room temperature the next day. The PVDF membranes were washed three times in Tris-buffered saline 0.1% Tween 20 (TBST; 3 × 10 min). Then each secondary antibody was incubated with the PVDF membrane at room temperature for 2 h. The PVDF membranes were washed three times in TBST (3 × 10 min). The membranes were then developed with a GE detection system. All bands were analyzed using Image-Pro Plus6.0 software. GAPDH was used as an internal control. Primary antibodies for this study were as follows:

GAPDH (1:5000, KC-5G4, KangChen, Shanghai, China); HDAC1(1:1000, 345898, Cell Signaling, Danvers, MA, USA); HDAC2 (1:1000, 5133S, Cell Signaling); HDAC3 (1:500, WL02946, Wanleibio, Shen Yang, China); HDAC6 (1:1000, 7612S, Cell Signaling); 4EBP (1:500, 9644, Cell Signaling); phosphorylation of 4EBP (P-4EBP, 1:500, 2855, Cell Signaling); P70 ribosomal protein S6 kinase (P70 S6, 1:500, 2708, Cell Signaling); phospho-p70 S6 Kinase (Thr389)(1:500, 9234, Cell Signaling); FOXO1 (1:500, 2880, Cell Signaling); phospho-FOXO1 (Ser256)(1:500, 9461, Cell Signaling); FOXO3(75D8) (1:500, 2497, Cell Signaling), phospho-FOXO3 (Ser253) (1:500, 9466, Cell Signaling), mitochondrial E3 ubiquitin protein ligase 1 (MUL1, 1:500, 16133-1-AP, Proteintech, Rosemont, IL, USA); TRIM63 (1:500, 55456-1-AP, Proteintech), FBXO32 (1:500, 12866-1-AP, Proteintech); LC3B (1:500, 2775, Cell Signaling); sequestosome1, P62 (1:500, P0067, Sigma-Aldrich); MEF2C (1:500, 5030, Cell Signaling); MYOD (1:500, 13812, Cell Signaling), MYH (1:500, C-12117, Santa Cruz Biotechnology, Dallas TX, USA); paired-like homeodomain transcription factor 1, PITX1 (1:500, H00005307-D01P, Abnova); MYBPC2 (1:500, PAB19214, Abnova, Tapei, Taiwan); LDB3 (1:500, PA5-30434, Thermo); P2RX7 (1:500, 11144-1-AP, Proteintech); caspase 9 (1:500, 9508, Cell Signaling); cleaved caspase 3 (1:500, 9661, Cell Signaling); NLRP3 (1:500, ab91413, Abcam); ASC (1:500, WL02462, Wanleibio); cleaved caspase 1 p20 (1:500, WL02996a, Wanleibio); cleaved IL-1β (1:500, 52,718, Cell Signaling).

2.5. Immunohistochemistry

Gas muscles were dissected and fixed in 4% paraformaldehyde for 24 h, embedded in paraffin, and cut into cross-sections (4 μm thick). Sections were deparaffinized in xylene and ethanol, hydrated and incubated with 3% H2O2 in methanol for 30 min at room temperature to block endogenous peroxidase. They were then washed three times in phosphate buffered saline (PBS; 3 × 5 min) and incubated with normal fetal bovine serum for 30 min at room temperature, and then with primary antibodies at 4 °C overnight. Sections were washed three times with PBS (3 × 10 min), then incubated with reagent A (KIT-9922, Maxim Biotechnologies, Rockville, MD, USA) for 15 min at room temperature and washed 3 times with PBS (3 × 5 min). Sections were incubated with reagent B (KIT-9922, Maxim Biotechnologies) for 30 min and washed three times with PBS (3 × 5 min), following by incubation with DAB (zli-9017, ZSGB-Biotechnologies). Negative controls were obtained by omitting the primary antibody. The sections were viewed under a Nikon Ni upright microscope using bright-field microscopy with 40× objective lenses and photographed using Nis-Elements software. Primary antibodies for this study were as follows:

HDAC1 (1:100); HDAC2 (1:100); MUL1 (1:50); FBXO32 (1:50); MEF2C (1:50); MYOD (1:50); PITX1 (1:50); MYBPC2 (1:50); LDB3 (1:50); P2RX7 (1:50); caspase 9 (1:50); cleaved caspase 3 (1:50); NLRP3 (1:50); ASC (1:50); cleaved caspase 1 p20 (1:50); cleaved IL-1β (1:50).

2.6. Statistical analyses

The data are presented as the mean ± standard error of the mean (SEM), with $P < 0.05$ indicating statistical significance. A two-tailed two-sample Student's *t*-test of unequal variance or one-way analysis or two-way ANOVA of variance was appropriate performed using GraphPad Prism 7.0.

3. Results

3.1. Impact of cigarette smoke exposure on muscle structure

Female C57BL/6 mice were exposed to room air or CS for 10, 20, 30 and 40 days, respectively, at least five mice in each group. Whole body mass increased in a time-dependent manner after exposure to room air, but time-dependently decreased after CS exposure (Fig. 1A, D). Gas muscle weight was significantly reduced in mice exposed to CS for 10, 20, 30 and 40 days, respectively, compared to that of mice exposed to room air (Fig. 1B, E). The weight of the TA was not significantly affected after 10 days of exposure to CS, but was significantly reduced after 20 and 30 days CS exposure, and especially after 40 days (Fig. 1B, F). The Tri muscle weight was identical to that of the TA (Fig. 1B, G). Histological analysis of the Gas from mice (CS exposure for 40 days) showed that the percentage of fibers with centralized nuclei increased in CS-exposed mice (Fig. 1C, H). These results indicated that CS exposure induced skeletal muscle atrophy and myofiber abnormality.

3.2. Exposure to CS resulted in HDAC1/2 protein upregulation and aberrations in protein turnover

Protein synthesis and degradation are associated with maintaining a balance in protein turnover in skeletal muscle; skeletal muscle atrophy occurs when protein degradation exceeds protein synthesis. HDACs and FOXO play important roles in protein synthesis and degradation. We found that HDAC1/2 increased while HDAC3/6 remained unchanged in the Gas of mice treated with CS for 40 days (Fig. 2A). This suggests that HDAC1/2 may participate in skeletal muscle atrophy induced by CS exposure. At the same time, the protein levels of p-FOXO1/FOXO1 and p-FOXO3/FOXO3 both increased after CS exposure compared to levels of the control group (Fig. 2B, C). This suggests that CS exposure inhibited the activation of FOXO1/3 in the Gas. In addition, proteins associated with protein synthesis–4EBP, p70, and their phosphorylated protein levels–were examined by western blot. The protein level of p-4EBP/4EBP and p-p70/p70 were found to be increased after CS exposure compared to levels of the control group (Fig. 2D, E). This indicated that protein synthesis was upregulated after CS exposure.

The degradation of proteins was also detected. Protein degradation is mediated by two typically conserved pathways: the ubiquitin–proteasome and autophagy lysosomal systems. After CS exposure, the expression of E3 ligase (TRIM63, FBXO32 and MUL1) was increased after CS exposure (Fig. 2F). This suggested that the ubiquitin–proteasome system is involved in skeletal muscle atrophy caused by CS exposure. The autophagy-associated protein, LC3BII, decreased after CS exposure for 10, 30 and 40 days but increased after 20 days compared to levels in respective control groups (Fig. 2G). This indicated that the formation of autophagosomes was inhibited after CS exposure for 10, 30 and 40 days, but was promoted after CS exposure for 20 days. The autophagy-associated protein, P62, decreased after CS exposure for 10 days and increased after CS exposure for 20, 30 and 40 days (Fig. 2G). This suggested that autophagic flow was blocked after 10 days of CS exposure and was upregulated after 20, 30 and 40 days of CS exposure. The protein level of LC3B II and P62 indicated that the impact of CS exposure on autophagy was not constant. Overall, the above results suggested that the inhibition of FOXO1/3 did not participate in inhibiting the ubiquitin–proteasome system but upregulating protein synthesis in the Gas of mice treated with CS for 40 days.

3.3. Exposure to CS resulted in the upregulation of markers of muscle fiber differentiation

Muscle fiber differentiation is essential to skeletal muscle formation, which is found to be abnormal in many muscle pathologies [20,21]. Markers of muscle fiber differentiation were detected by western blot after CS exposure for 40 days. Compared to the control group, markers of early (MEF2C, MYOD) and terminal differentiation (total MYH) all increased following CS exposure. Moreover, the expression of PITX1, an upstream regulatory protein of MEF2C, was also increased (Fig. 3A). The above results indicated that CS exposure upregulated markers of muscle fiber differentiation.

3.4. Exposure to CS resulted in upregulation of cytoskeletal proteins

Cytoskeletal proteins take part in maintaining cellular architecture and internal organization [22]. In our previous work, we found that some cytoskeletal proteins (MYBPC2 and LDB3) were involved in the formation of skeletal muscle pathological changes in FHL1 knockout (KO) mice and in differentiated C2C12 myoblasts after 17β-estradiol exposure [23,24]. Therefore, protein levels of MYBPC2 and LDB3 were evaluated by western blot after CS exposure for 40 days. We found that after CS exposure, MYBPC2 and LDB3 were both increased (Fig. 3B). This suggests that MYBPC2 and LDB3 were involved in skeletal muscle abnormalities caused by CS exposure.

3.5. CS exposure upregulated apoptosis and pyroptosis mediated by P2RX7

P2RX7 and markers associated with apoptosis (caspase 9 and cleaved caspase 3) and pyroptosis (NLRP3, ASC, cleaved caspase 1 and IL-1β) were investigated by western blot. P2RX7 was increased in the Gas of mice treated with CS (Fig. 3C). In addition, caspase 9 and cleaved caspase 3 were both increased in the Gas of mice treated with CS (Fig. 3C). At the same time, CS exposure triggered NLRP3, ASC, cleaved caspase 1 and IL-1β to increase in the Gas (Fig. 3D). The results indicated that P2RX7-mediated apoptosis and pyroptosis were upregulated in the CS-treated Gas of mice, which were associated with skeletal muscle atrophy after CS exposure.

3.6. TSA restored skeletal muscle weight loss and abnormal muscle fiber structure caused by CS exposure

HDACs have recently come into focus as a therapeutic target. However, the effects of TSA, a HDAC inhibitor, on skeletal muscle alterations induced by CS exposure have not been demonstrated. HDAC1/2 upregulation was shown in the Gas of mice treated with CS. Thus, in this study, mice were exposed to CS for 120 min, twice daily, and injected intraperitoneally with TSA (0.6 mg/kg body weight on alternate days) for 40 days. We found that TSA attenuated the loss of body weight (Fig. 4A) and wet weight of skeletal muscle (Fig. 4B) induced by CS exposure. Furthermore, TSA reduced the percentage of fibers showing centralized nuclei caused by CS exposure (Fig. 4C). These results

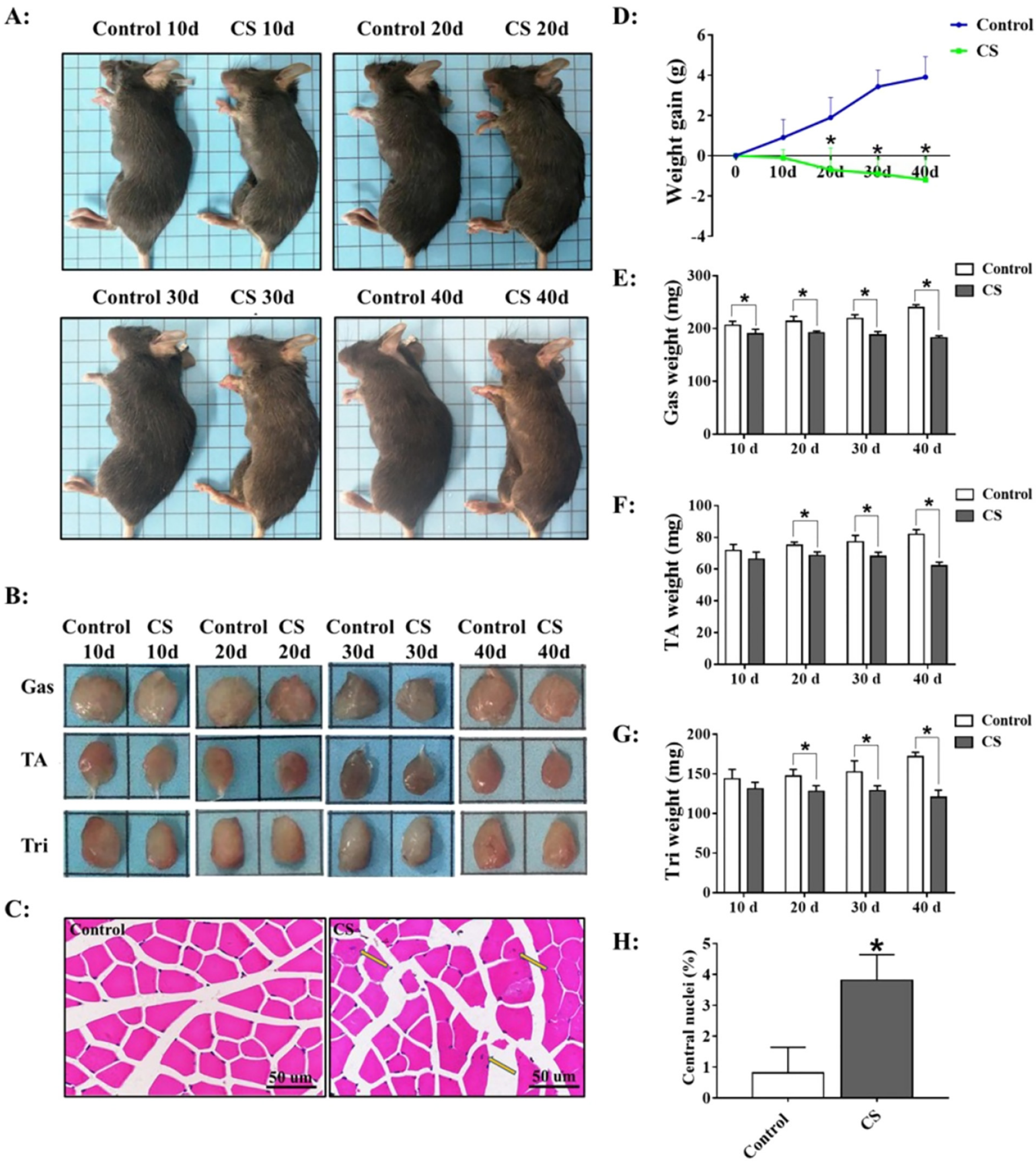

Fig. 1. CS exposure decreased whole body weight and skeletal muscle mass, and changed muscle fiber structure. A, D: Compared with mice exposed to room air, the body weights of mice exposed to cigarette smoke (CS) decreased in a time-dependent manner. B, E, F, G: CS exposure decreased gastrocnemius (Gas), tibialis anterior (TA) and triceps (Tri) wet weights compared to controls. C: Histological analysis of the Gas muscle from mice (CS exposure for 40 days) by hematoxylin and eosin (HE) stain showing an increased percentage of fibers with centralized nuclei in CS-exposed mice. The arrows point to fibers with centralized nuclei. H: The number of muscle fibers with central nuclei in the Gas was quantified as a percentage of the total number of muscle fibers analyzed. Data are shown as the mean ± SEM ($n \geq 5$). $^{*}P < 0.05$.

indicated that TSA inhibited muscle atrophy and histomorphological alterations induced by CS exposure.

3.7. *TSA inhibited the upregulation of HDAC1/2 and ubiquitin degradation induced by CS exposure*

TSA inhibited muscle atrophy and Gas histomorphological alterations induced by CS exposure, but the mechanism was not clear. We found that markers of ubiquitin degradation were upregulated in the Gas of mice treated with CS for 40 days. It was therefore necessary to measure the level of ubiquitin degradation after TSA exposure. TSA was found to significantly restore the expression of HDAC1/2 and markers of ubiquitin degradation induced by CS exposure (Fig. 5). These results indicated that TSA inhibited muscle atrophy and histomorphological alterations induced by CS exposure and that the TSA effect may be associated with a reduction of ubiquitin degradation via HDAC1/2 inhibition.

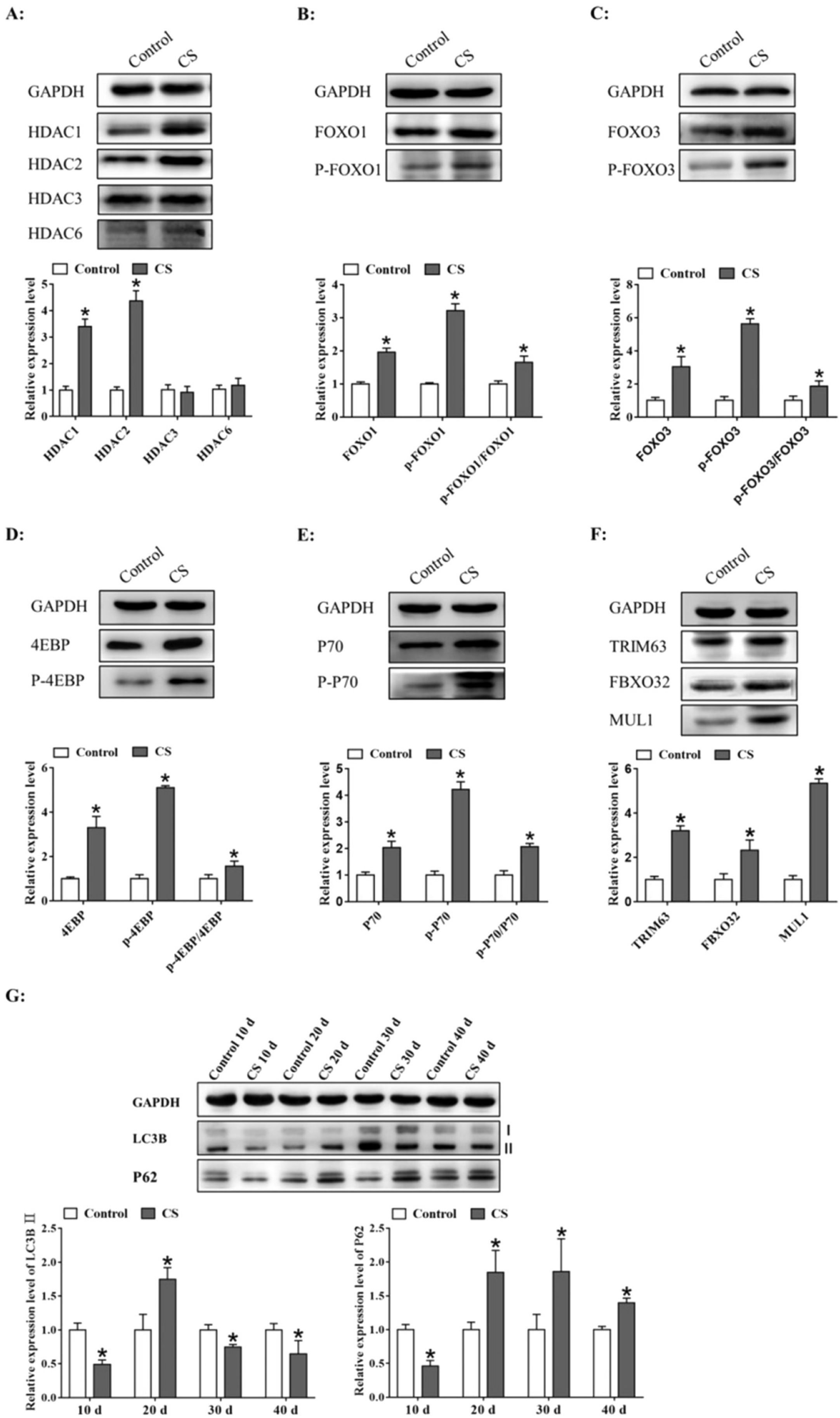

(caption on next page)

Fig. 2. Exposure to CS resulted in HDAC1/2 upregulation and aberrations in protein turnover. After female C57BL/mice were exposed to cigarette smoke (CS) for 40 days, proteins associated with protein turnover were examined by western blot. A: CS exposure upregulated HDAC1/2 proteins but did not affect the protein levels of HDAC3 and HDAC6. B, C: CS exposure inhibited the activation of FOXO1/3 in the Gas. D, E: CS exposure promoted protein synthesis (4EBP, P70). F: CS exposure promoted ubiquitin degradation (TRIM63, FBXO32 and MUL1). G: The effect of CS exposure on autophagy was not constant. The autophagy-associated protein, LC3BII, decreased after CS exposure for 10, 30 and 40 days but increased after 20 days compared to respective control groups. The autophagy-associated protein, P62, decreased after CS exposure for 10 days but increased after 20, 30 and 40 days compared to respective control groups. Data are shown as the mean ± SEM ($n \geq 5$). $^*P < 0.05$.

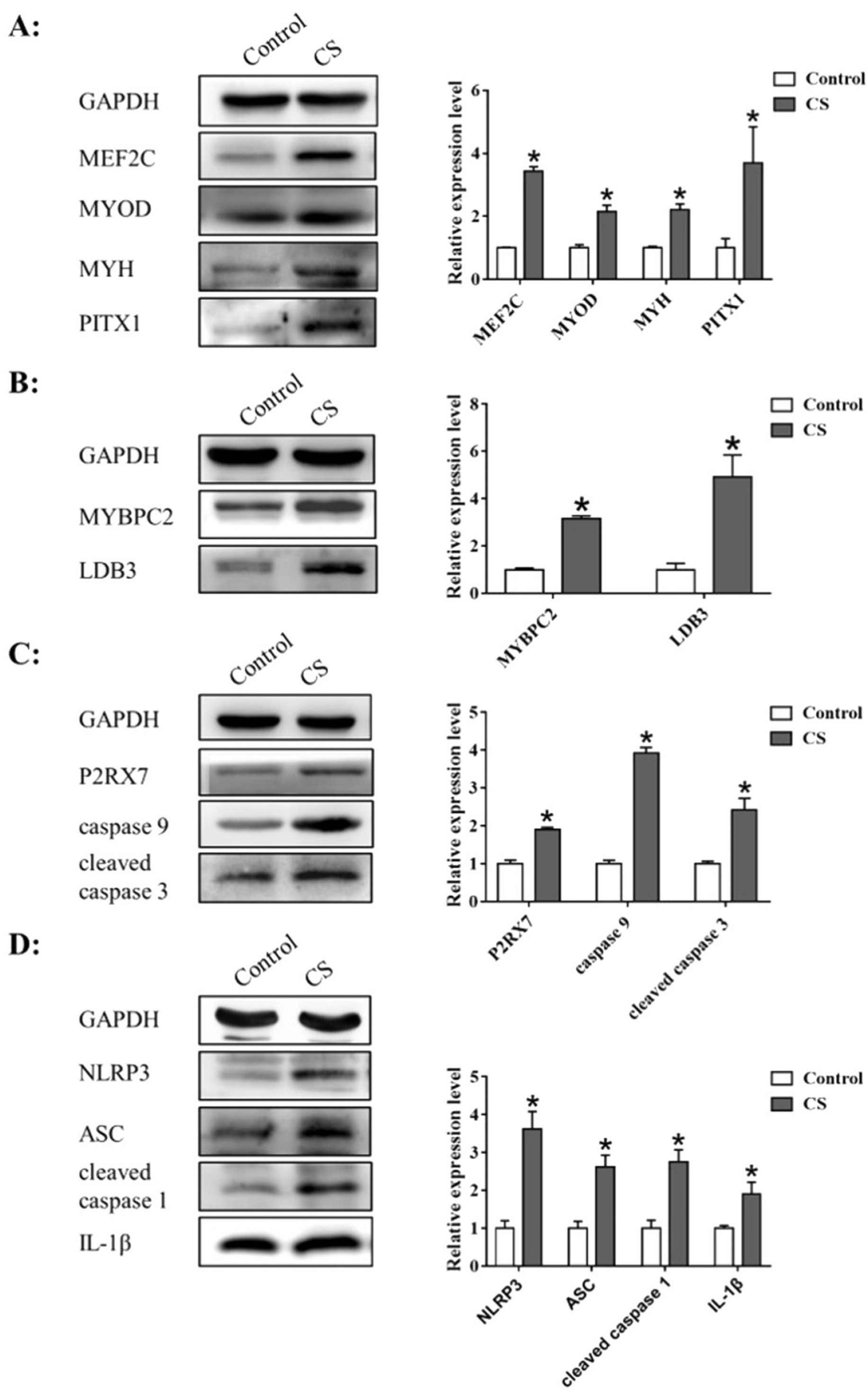

Fig. 3. CS exposure upregulated markers of muscle fiber differentiation, cytoskeletal proteins, apoptosis and pyroptosis. A: Western blot analysis of markers for muscle fiber differentiation in controls and cigarette smoke (CS)–treated gastrocnemius (Gas) of mice. Statistical analysis indicated that MEF2C, MYOD, MYH and PITX1 were significantly increased in the muscle of mice treated with CS. B: Western blot analysis of markers for cytoskeletal proteins in the Gas of control and CS exposed mice. Statistical analysis indicated MYBPC2 and LDB3 were markedly increased in the muscle of mice treated with CS. C: Western blot analysis of markers for apoptosis and P2RX7 in the Gas of control and CS exposed mice. Statistical analysis indicated P2RX7, caspase 9 and cleaved caspase 3 were significantly increased in the muscle of mice treated with CS. D: Western blot analysis of protein markers of pyroptosis in the Gas of control and CS exposed mice. Statistical analysis indicated NLRP3, ASC, cleaved caspase 1 and interleukin (IL)-1β were markedly increased in the muscle of mice treated with CS. Data are shown as the mean ± SEM ($n \geq 5$). $^*P < 0.05$.

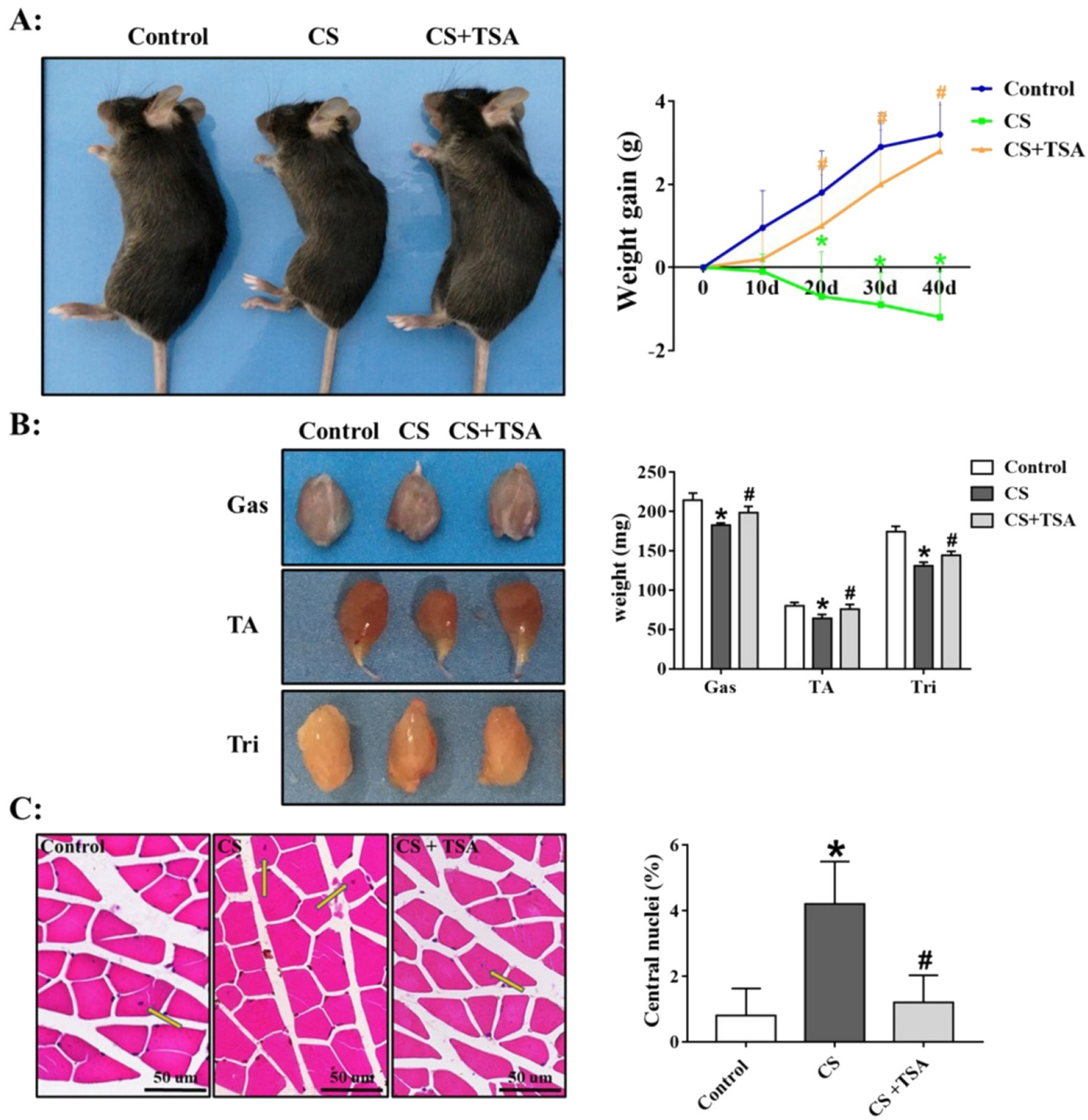

Fig. 4. TSA restored skeletal muscle weight loss and abnormal muscle fiber structure caused by CS exposure. Female C57BL/mice were divided into three groups that included a Control group, cigarette smoke (CS) exposure group and CS exposure + trichostatin A (TSA). All mice were weighed every day. After 40 days of CS exposure, at least five mice in each group were selected and the Gas, TA and Tri muscles of each animal were weighed. A: TSA attenuated the loss of body weight caused by exposure to CS. B: TSA restored the loss of skeletal muscle mass caused by CS exposure. C: TSA reduced the percentage of fibers with centralized nuclei caused by CS exposure. Data are shown as the mean ± SEM ($n \geq 5$). $^{*}P < 0.05$ (Control vs. CS), $^{\#}P < 0.05$ (CS vs. CS + TSA).

3.8. *TSA inhibited markers of muscle fiber differentiation and cytoskeletal proteins induced by CS exposure*

CS exposure increased markers of fiber differentiation and cytoskeletal proteins (Fig. 3A, B). It was therefore necessary to investigate whether HDAC1/2 regulated fiber differentiation and cytoskeletal proteins exposed to CS. We found that TSA significantly inhibited markers of muscle fiber differentiation (MEF2C, MYOD, MYH and PITX1; Fig. 6) and cytoskeletal proteins (MYBPC2 and LDB3; Fig. 7) induced by CS exposure. This indicated that TSA alleviated skeletal muscle atrophy caused by CS exposure and that the TSA effect may be associated with a reduction of markers of differentiation as well as cytoskeletal proteins via HDAC1/2 inhibition.

A: Western blot analysis of cytoskeletal proteins (MYBPC2 and LDB3) in Control, cigarette smoke (CS)-treated and CS + trichostatin A (TSA)–treated gastrocnemius (Gas) of mice. Statistical analysis indicated that TSA effectively downregulated protein levels of MYBPC2 and LDB3 induced by CS exposure. B, C: Immunohistochemical analysis of cytoskeletal proteins (MYBPC2 and LDB3) in Control, CS-treated and CS + TSA–treated Gas of mice. Statistical analysis indicated that TSA effectively downregulated protein levels of MYBPC2 and LDB3 induced by CS exposure. Data are shown as the mean ± SEM ($n \geq 5$). $^{*}P < 0.05$ (Control vs. CS), $^{\#}P < 0.05$ (CS vs. CS + TSA).

3.9. *TSA decreased the upregulation of apoptosis and pyroptosis mediated by P2RX7 and caused by CS exposure*

Our results displayed that P2RX7, markers of apoptosis and pyroptosis were all increased after CS exposure (Fig. 3C, D). Those results suggested that apoptosis and pyroptosis had roles in skeletal muscle atrophy and muscle abnormalities induced by CS exposure. However, the effect of TSA on apoptosis and pyroptosis was undetermined. Protein levels of P2RX7, and markers of apoptosis (caspase 9 and cleaved caspase 3) and pyroptosis (NLRP3, ASC, cleaved caspase 1 and IL-1β)

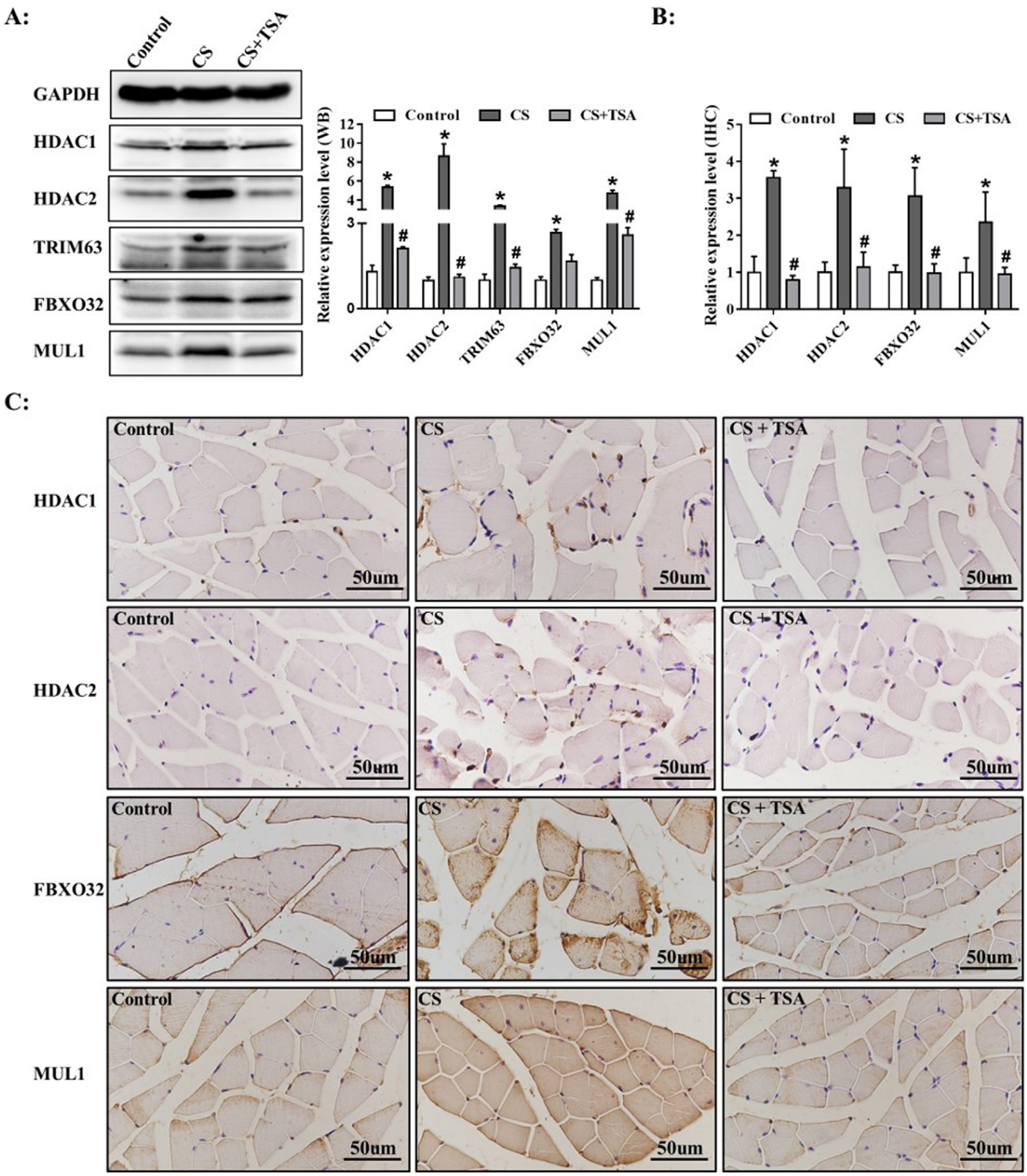

Fig. 5. TSA inhibited the upregulation of HDAC1/2 and ubiquitin degradation induced by CS exposure. A: Western blot analysis of HDAC1/2 and proteins associated with ubiquitin degradation (TRIM63, FBXO32 and MUL1) in Control, cigarette smoke (CS)-treated and CS + trichostatin A (TSA)–treated gastrocnemius (Gas) of mice. Statistical analysis indicated that TSA effectively inhibited the upregulation of HDAC1/2, TRIM63, FBXO32 and MUL1 proteins caused by CS exposure. B, C: Immunohistochemistry analysis of HDAC1/2 and proteins associated with ubiquitin degradation (FBXO32 and MUL1) in Control, CS-treated and CS + TSA–treated Gas of mice. Statistical analysis indicated that TSA effectively inhibited the upregulation of HDAC1/2, FBXO32 and MUL1 proteins caused by CS exposure. Data are shown as the mean ± SEM ($n \geq 5$). $^{*}P < 0.05$ (Control vs. CS), $^{\#}P < 0.05$ (CS vs. CS + TSA).

were evaluated by western blot and immunohistochemistry after TSA exposure. TSA effectively downregulated P2RX7 protein in the Gas induced by CS exposure. Furthermore, TSA attenuated the upregulation of apoptosis (Fig. 8) and pyroptosis (Fig. 9) caused by CS exposure. This suggested that TSA alleviated skeletal muscle atrophy caused by CS exposure and that this effect may be associated with a reduction of apoptosis and pyroptosis mediated by P2RX7 via HDAC1/2 inhibition.

4. Discussion

Previous studies have shown that CS exposure contribute to the development of skeletal muscle atrophy in COPD [25,26]. CS is also associated with sarcopenia or age-related muscle atrophy and the loss of muscle strength [27–29]. In addition, Krüger et al. found that exposure to CS caused decreased exercise capacity and inflammation, which were associated with skeletal muscle atrophy [30]. However, the molecular mechanisms underlying skeletal muscle atrophy induced by

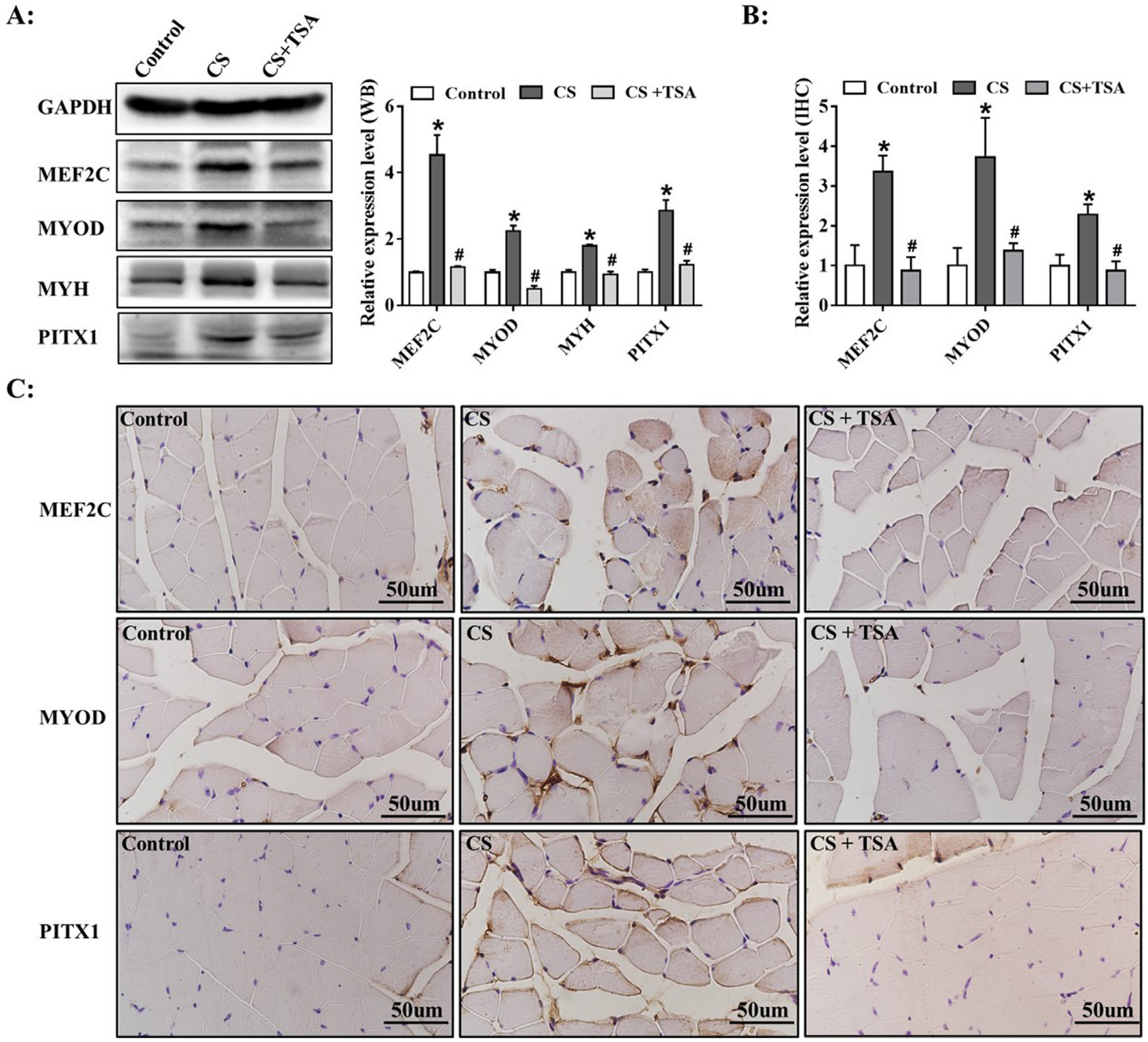

Fig. 6. TSA inhibited markers of muscle fiber differentiation caused by CS exposure. A: Western blot analysis of markers of muscle fiber differentiation (MEF2C, MYOD, MYH and PITX1) in Control, cigarette smoke (CS)-treated and CS + trichostatin A (TSA)–treated gastrocnemius (Gas) of mice. Statistical analysis indicated that TSA effectively reduced the activity of MEF2C, MYOD, MYH and PITX1 induced by CS exposure. B, C: Immunohistochemical analysis of markers of muscle fiber differentiation (MEF2C, MYOD and PITX1) in Control, CS-treated and CS + TSA–treated Gas of mice. Statistical analysis indicated that TSA effectively reduced protein levels of MEF2C, MYOD and PITX1 induced by CS exposure. Data are shown as the mean ± SEM ($n \geq 5$). $^{*}P < 0.05$ (Control vs. CS), $^{\#}P < 0.05$ (CS vs. CS + TSA).

CS remained elusive. In this study, muscle atrophy and structural changes caused by CS exposure were investigated and the molecular mechanisms underlying this process explored. Whole-body exposure of mice to CS was used in this study, as described in our previous study [19]. We showed that CS exposure twice daily for 40 days triggered the loss of body weight and skeletal muscle (Gas, TA and Tri) wet weight, and induced Gas histomorphological alterations. The percentage of fibers with centralized nuclei increased in CS-exposed mice compared to mice exposed to room air. This suggested that CS exposure caused skeletal muscle atrophy and structural abnormalities. Therefore, exploring the mechanisms involved in CS-induced skeletal muscle damage was important.

HDACs remove acetyl groups from target proteins, and have played an essential role in regulating skeletal muscle atrophy in several pathophysiological conditions [31,32]. The specific knockout of HDAC1/2 in skeletal muscle caused a proportion of mice pups to die during the perinatal period, with mitochondrial abnormalities and sarcomere degeneration evident [7]. Skeletal muscle atrophy is caused by the inhibition of protein synthesis and the upregulation of protein degradation that includes the ubiquitin–proteasome system and autophagy. HDAC1 promotes muscle atrophy by increasing the FOXO-dependent transcription of target genes involved in the ubiquitin–proteasome pathway (TRIM63 and FBXO32), autophagy (LC3) and by inhibiting protein synthesis (4EBP) [8]. Therefore, we hypothesized that HDACs promoted skeletal muscle atrophy caused by CS exposure by regulating FOXO-dependent protein synthesis and degradation. Hu et al. observed that after exposure to side-stream smoke 1 h daily for 40 days, autophaglysosome formation became defective in the hearts of mice [33]. However, Ting et al. reported that after environmental exposure to tobacco smoke twice daily (morning and afternoon) for 6 weeks, autophagy increased in the hearts of mice [34]. We suspected that the upregulation or downregulation of autophagy by CS was due to different exposure times. Therefore, in this study, autophagy was evaluated in the Gas of mice after CS exposure for 10, 20, 30 and 40 days, while other protein levels were measured at only 40 days after CS exposure. We found that HDAC1/2 increased and HDAC3/6 remained unchanged in the Gas of mice treated with CS. This suggests that HDAC1/2 may participate in Gas histomorphological alterations

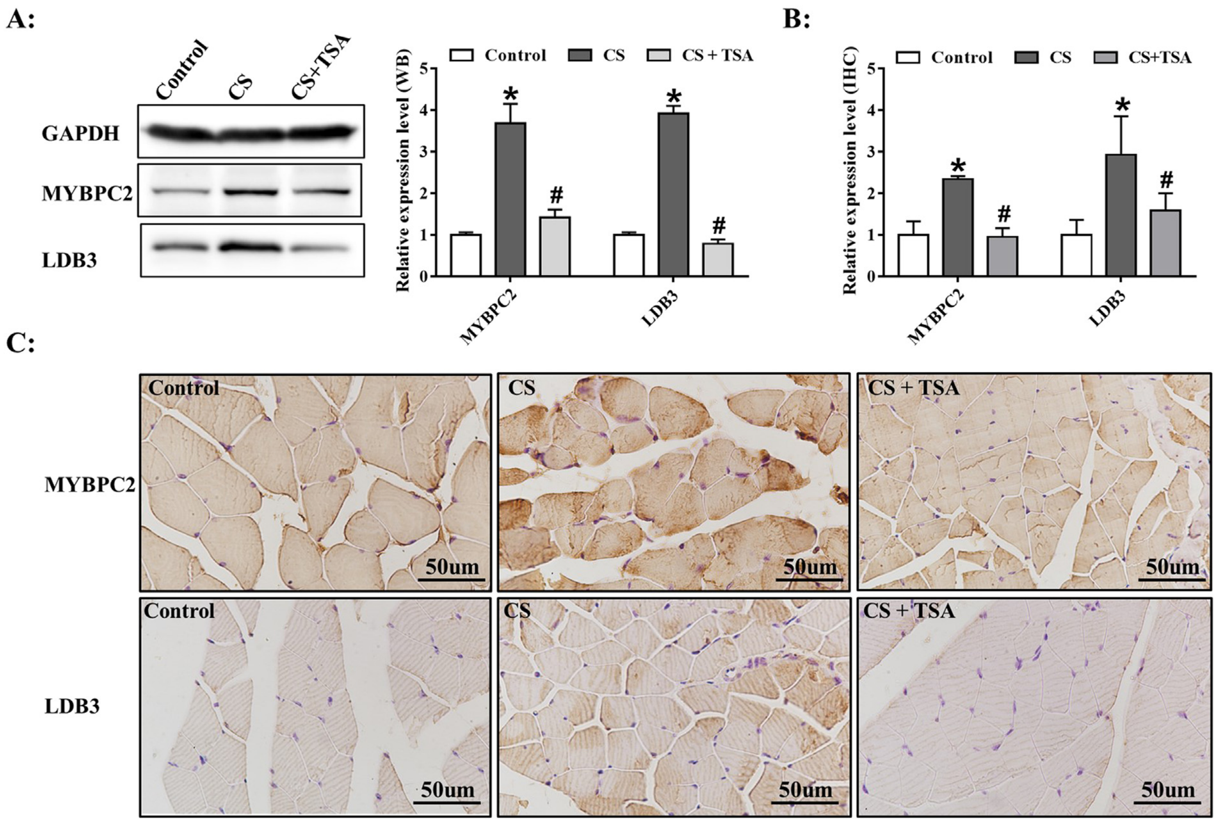

Fig. 7. TSA inhibited cytoskeletal proteins upregulated by CS exposure.

induced by CS exposure. At the same time, the protein level of p-FOXO1/FOXO1 and p-FOXO3/FOXO3 were both upregulated. This result is inconsistent with the study of Beharry et al. [8]. Some studies have shown that the phosphorylation of FOXOs was also regulated by other signaling pathways including Akt signaling pathway [35,36]. Therefore we suspect that after CS exposure, other regulators may promote the protein level of p-FOXO1 and p-FOXO3. What is more, protein synthesis and the ubiquitin–proteasome pathway were upregulated after CS exposure for 40 days. Interestingly, the effect of CS exposure on autophagy levels was not constant as we suspected. The autophagy-associated protein, LC3B II, was decreased after CS exposure for 10, 30 and 40 days, but increased after 20 days compared to respective control groups. The autophagy-associated protein, P62, decreased after 10 days CS exposure and increased after 20, 30 and 40 days CS exposure compared to respective control groups. These results indicated that autophagy and protein synthesis processes were not involved in skeletal muscle atrophy after 40 days of CS exposure. However, CS exposure may promote ubiquitination by activating HDAC1/2 to cause skeletal muscle atrophy. What is more, CS exposure upregulated markers of muscle fiber differentiation (MEF2C, MYOD, MYH and PITX1), cytoskeletal proteins (MYBPC2 and LDB3), apoptosis (caspase 9 and cleaved caspase 3) and pyroptosis (NLRP3, ASC, cleaved caspase 1, IL-1β). The above proteins may also be involved in CS-induced skeletal muscle atrophy. Therefore, HDAC1/2 came into focus as a therapeutic target. Furthermore, the effects of TSA, an HDAC inhibitor, on Gas histomorphological alterations and the upregulation of proteins involved in ubiquitination, muscle fiber differentiation, cytoskeletal proteins, apoptosis and pyroptosis induced by CS exposure were further investigated.

As our data showed, TSA attenuated the loss of body weight and Gas wet weight and reduced percentage of fibers with centralized nuclei induced by CS exposure. Furthermore, TSA effectively inhibited HDAC1/2 protein upregulation and reduced protein levels of the ubiquitin–proteasome pathway caused by CS exposure. These results indicated that TSA inhibited muscle atrophy induced by CS exposure and that the TSA effect may be associated with a reduction of ubiquitin degradation via HDAC1/2 inhibition.

Muscle fiber differentiation is a crucial stage in determining skeletal muscle formation. In our previous research, we found that markers of early (MEF2C and MYOD1) and terminal differentiation (MYH) were both upregulated in FHL1 KO mice with abnormal skeletal muscle morphology [23]. MEF2C and MYOD also involve in the regeneration of skeletal muscle damage [37,38]. Moreover, the over-expression of PITX1, the upstream regulatory protein of MEF2C, leads to myofiber atrophy and muscular dystrophy [39]. Previous studies have demonstrated that HDAC1 binds directly to MEF2C and MYOD to regulate cell differentiation [40,41]. In our work, skeletal muscle differentiation–related proteins (MEF2C, MYOD, MYH and PITX1) all increased in the Gas of mice treated with CS and were effectively inhibited by TSA. These results indicated that TSA inhibited muscle atrophy induced by CS exposure and that the effect of TSA may be associated with a reduction in markers of muscle fiber differentiation or regeneration via HDAC1/2 inhibition.

Additionally, cytoskeletal proteins take part in maintaining cellular architecture and internal organization [22]. MYBPC2 and LDB3, members of the cytoskeletal family of proteins, are involved in many pathological changes in muscle. MYBPC proteins regulate muscle structure and function, which interact with the head region of myosin and actin to maintain thick filament stability and regulate contractility [42]. LDB3 is essential for maintaining skeletal muscle structural integrity and function [43]. Abnormal splicing of LDB3 plays an essential role in myotonic dystrophies type 1 and 2 [44]. In our previous work, we found that MYBPC2 and LDB3 were involved in the formation of pathological changes in the skeletal muscle of FHL1 KO mice and in differentiated C2C12 myoblasts after 17β-estradiol exposure [23,24]. Thus, we reasoned that cytoskeletal proteins may be involved in skeletal muscle atrophy caused by CS exposure. Our results showed that MYBPC2 and LDB3 proteins were upregulated in the Gas of mice

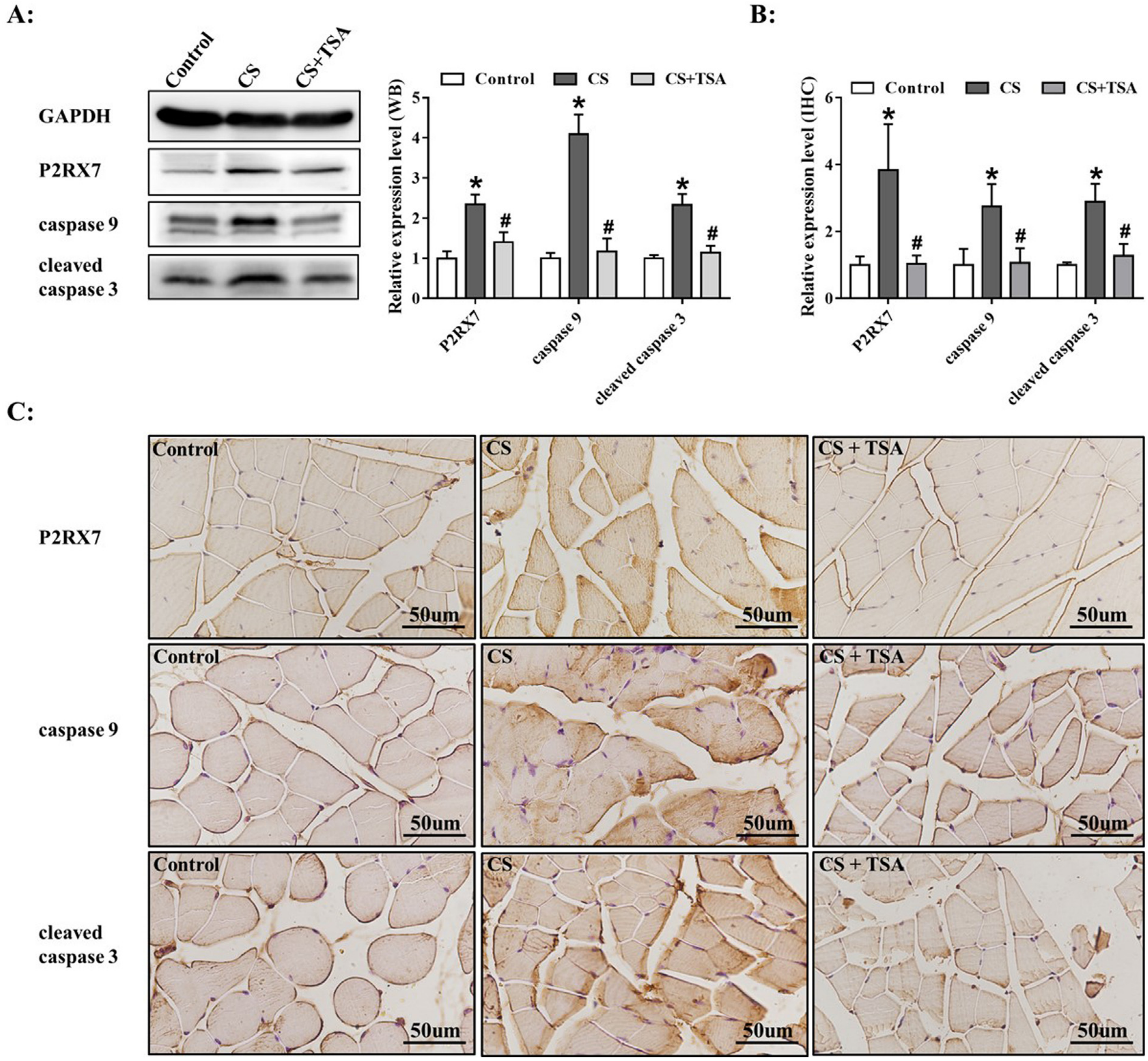

Fig. 8. TSA decreased apoptosis mediated by P2RX7 and caused by CS exposure. A: Western blot analysis of markers of apoptosis (caspase 9 and cleaved caspase 3) in gastrocnemius (Gas) of mice treated with cigarette smoke (CS) and trichostatin A (TSA). Statistical analysis indicated that TSA decreased the expression of caspase 9 and cleaved caspase 3 induced by CS exposure. B, C: Immunohistochemistry analysis of markers of apoptosis (caspase 9 and cleaved caspase 3) in the Gas of mice treated with CS and TSA. Statistical analysis indicated that TSA lowered the protein expression of caspase 9 and cleaved caspase 3 induced by CS exposure. Data are shown as the mean ± SEM ($n \geq 5$). $^{*}P < 0.05$ (Control vs. CS), $^{\#}P < 0.05$ (CS vs. CS + TSA).

treated with CS and inhibited by TSA. This indicated that the upregulation of MYBPC2 and LDB3 proteins was involved in skeletal muscle atrophy caused by CS exposure and can be inhibited by TSA. The effect of TSA inhibition on the upregulation of MYBPC2 and LDB3 proteins may occur via HDAC1/2 inhibition.

What is more, the upregulation of P2RX7, an ATP-gated ion channel, induced muscle cell damage and pathology; the subsequent inhibition of P2RX7 improved muscle function in Duchenne muscular dystrophy [45]. P2RX7 also plays an important role in dystrophic myoblasts and myotubes [13]. The upregulation of P2RX7 needed high levels of extracellular ATP for dystrophic muscle cells and induced a number of mechanisms, including apoptosis and pyroptosis [13–15]. Zhang et al. reported that Gurigumu-13 GRGM-13 inhibited the oxidative stress-induced apoptosis of retinal ganglion cells by inhibiting the P2RX7/p38 MAPK pathway [46]. Apoptosis is also essential to various muscle pathologies. Cell apoptosis is an important mechanism underlying skeletal muscle dysfunction in patients with COPD. Mao et al. found that cell apoptosis were increased in a COPD rat model [16]. The upregulation of apoptosis was also involved in ageing-related muscle atrophy and denervation-induced muscle abnormalities [47]. In comparison, pyroptosis is also essential to skeletal muscle atrophy. NLRP3/IL-1β upregulation is an essential pathogenic mechanism in the inflammatory skeletal muscle atrophy of sepsis so that the inhibition of NLRP3/IL-1β relieved muscle atrophy [18]. Wang et al. reported that NLRP3 and caspase 1 were both upregulated in alveolar epithelial (A549) cells and bronchial epithelial (Beas-2B) cells following exposure to cigarette smoke extract [48]. However, whether P2RX7-mediated apoptosis and pyroptosis were involved in skeletal muscle abnormalities caused by CS was unclear. In this work, the upregulation of P2RX7-mediated apoptosis and pyroptosis was investigated in the Gas of mice treated with CS. We found that P2RX7, and markers of apoptosis (caspase 9 and cleaved caspase 3) and pyroptosis (NLRP3, ASC, cleaved caspase 1 and IL-1β) were all upregulated in the Gas of CS-exposed mice and that this was limited by TSA. Our studies suggested that TSA alleviated skeletal muscle atrophy caused by CS exposure and that the TSA effect may be associated with a reduction of apoptosis and pyroptosis mediated by P2RX7 via the inhibition of HDAC1/2.

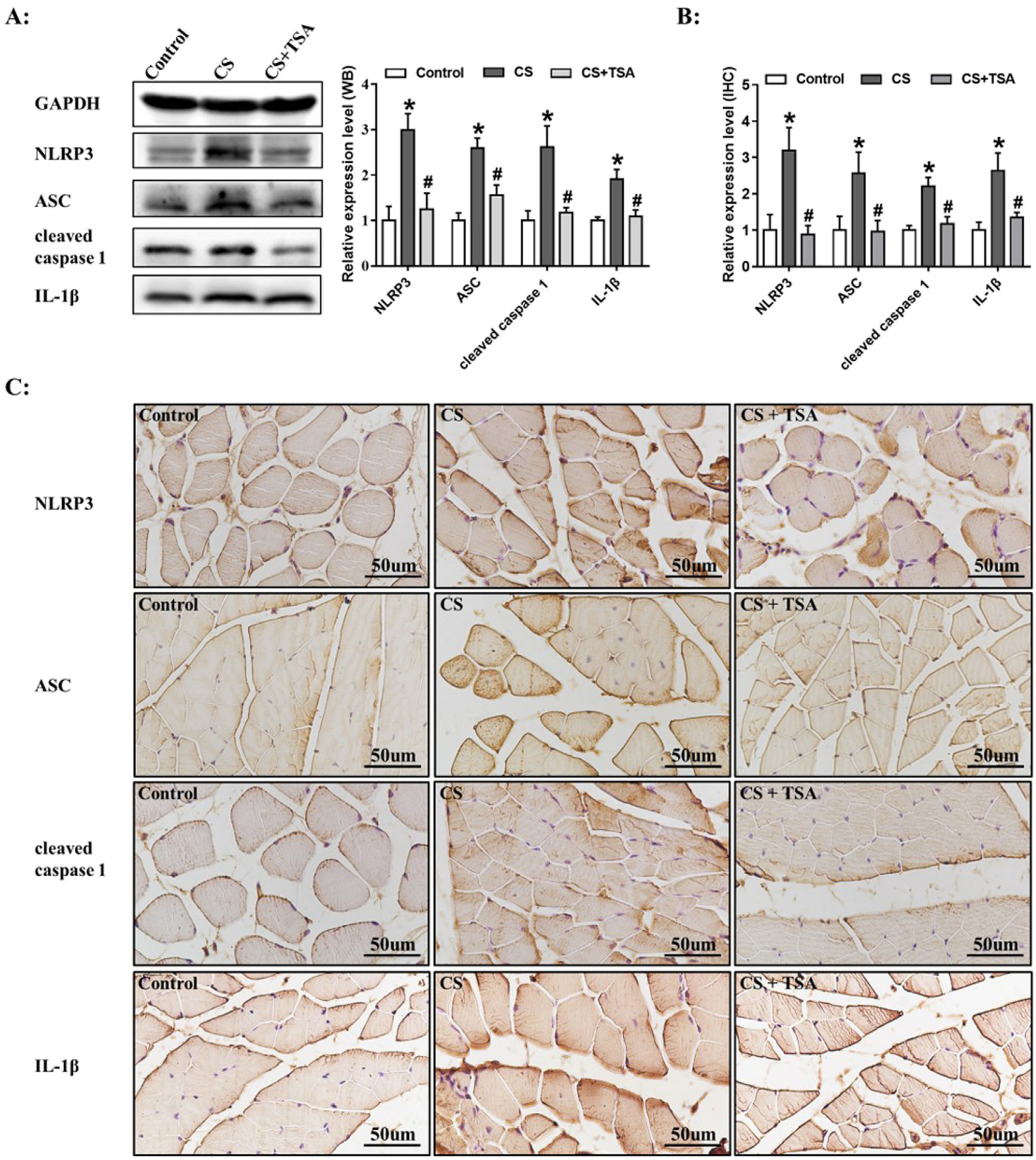

Fig. 9. TSA inhibited pyroptosis mediated by P2RX7 and caused by CS exposure. A: Western blot analysis of markers of pyroptosis (NLRP3, ASC, cleaved caspase 1 and interleukin [IL]-1β) in the gastrocnemius (Gas) of mice treated with cigarette smoke (CS) and trichostatin A (TSA). Statistical analysis indicated that TSA decreased the expression of NLRP3, ASC, cleaved caspase 1 and IL-β proteins induced by CS exposure. B, C: Immunohistochemistry analysis of markers of pyroptosis (NLRP3, ASC, cleaved caspase 1 and IL-1β) in the Gas of mice treated with CS and TSA. Statistical analysis indicated that TSA lowered the expression of NLRP3, ASC, cleaved caspase 1 and IL-1β proteins induced by CS exposure. Data are shown as the mean ± SEM (n ≥ 5). $^{*}P < 0.05$ (Control vs. CS), $^{\#}P < 0.05$ (CS vs. CS + TSA).

5. Conclusions

TSA may inhibit skeletal muscle atrophy and histomorphological alterations induced by CS exposure as shown by the downregulation of upregulated markers of ubiquitin degradation, muscle fiber differentiation or regeneration, cytoskeletal proteins, apoptosis and pyroptosis via the inhibition of HDAC1/2. Taken together , our data suggest that TSA may be a potential therapy for skeletal muscle atrophy associated with some diseases such as COPD and sarcopenia caused by CS.

Acknowledgments

We would like to express our gratitude to all participants of this study. This study was supported by the National Natural Science Foundation of China (81971459) and Liaoning Provincial Natural Science Foundation of China (2019-MS-361) .

Declaration of competing interests

The authors declare that there are no conflicts of interest.

Appendix A. Supplementary data

Supplementary data to this article can be found online at https://doi.org/10.1016/j.lfs.2019.116800.

References

[1] S. Basu, D. Stuckler, A. Bitton, et al., Projected effects of tobacco smoking on worldwide tuberculosis control: mathematical modelling analysis, BMJ 343 (2011) d5506 https://doi.org/10.1136/bmj.d5506.

[2] K. Tomoda, K. Kubo, K. Hino, et al., Branched-chain amino acid-rich diet improves skeletal muscle wasting caused by cigarette smoke in rats, J. Toxicol. Sci. 39 (2014) 331–337 https://doi.org/10.2131/jts.39.331.

[3] Q. Liu, W.G. Xu, Y. Luo, et al., Cigarette smoke-induced skeletal muscle atrophy is associated with up-regulation of USP-19 via p38 and ERK MAPKs, J. Cell. Biochem. 112 (2011) 2307–2316, https://doi.org/10.1002/jcb.23151.

[4] R.A. Rabinovich, J. Vilaró, Structural and functional changes of peripheral muscles in chronic obstructive pulmonary disease patients, Curr. Opin. Pulm. Med. 16 (2010) 123–133, https://doi.org/10.1097/MCP.0b013e328336438d.

[5] M. Steffl, R.W. Bohannon, M. Petr, et al., Relation between cigarette smoking and sarcopenia: meta-analysis, Physiol. Res. 64 (2015) 419–426.

[6] C. Choudhary, C. Kumar, F. Gnad, et al., Lysine acetylation targets protein complexes and co-regulates major cellular functions, Science 325 (2009) 834–840, https://doi.org/10.1126/science.1175371.

[7] V. Moresi, M. Carrer, C.E. Grueter, et al., Histone deacetylases 1 and 2 regulate autophagy flux and skeletal muscle homeostasis in mice, Proc. Natl. Acad. Sci. U. S. A. 109 (2012) 1649–1654, https://doi.org/10.1073/pnas.1121159109.

[8] A.W. Beharry, P.B. Sandesara, B.M. Roberts, et al., HDAC1 activates FoxO and is both sufficient and required for skeletal muscle atrophy, J. Cell Sci. 127 (2014) 1441–1453, https://doi.org/10.1242/jcs.136390.

[9] S. Dupre-Aucouturier, J. Castells, D. Freyssenet, et al., Trichostatin A, a histone deacetylase inhibitor, modulates unloaded-induced skeletal muscle atrophy, J. Appl. Physiol. 119 (2015) (1985) 342–351, https://doi.org/10.1152/japplphysiol.01031.2014.

[10] Y.E. Yoo, C.P. Ko, Treatment with trichostatin A initiated after disease onset delays disease progression and increases survival in a mouse model of amyotrophic lateral sclerosis, Exp. Neurol. 231 (2011) 147–159, https://doi.org/10.1016/j.expneurol.2011.06.003.

[11] M. Bosch-Marce, C.D. Wee, T.L. Martinez, et al., Increased IGF-1 in muscle modulates the phenotype of severe SMA mice, Hum. Mol. Genet. 20 (2011) 1844–1853, https://doi.org/10.1093/hmg/ddr067.

[12] O.C. Steinbac, A.P. Wolffe, R.A. Rupp, Histone deacetylase activity is required for the induction of the MyoD muscle cell lineage in Xenopus, Biol. Chem. 381 (2000) 1013–1016, https://doi.org/10.1515/bc.2000.124.

[13] C.N. Young, A. Sinadinos, A. Lefebvre, et al., A novel mechanism of autophagic cell death in dystrophic muscle regulated by P2RX7 receptor large-pore formation and HSP90, Autophagy 11 (2015) 113–130, https://doi.org/10.4161/15548627.2014.994402.

[14] A.R. Lee, K. Hong, S.H. Choi, et al., Anti-apoptotic regulation contributes to the successful nuclear reprogramming using cryopreserved oocytes, Stem. Cell. Reports. 12 (2019) 545–556, https://doi.org/10.1016/j.stemcr.2019.01.019.

[15] R. Dang, X. Zhou, M. Tang, et al., Fish oil supplementation attenuates neuroinflammation and alleviates depressive-like behavior in rats submitted to repeated lipopolysaccharide, Eur. J. Nutr. 57 (2018) 893–906, https://doi.org/10.1007/s00394-016-1373-z.

[16] J. Mao, Y. Li, Bufei Jianpi granules reduce quadriceps muscular cell apoptosis by improving mitochondrial function in rats with chronic obstructive pulmonary disease, Evid. Based Complement. Alternat. Med. 2019 (2019) 1216305, , https://doi.org/10.1155/2019/1216305.

[17] B. De Paepe, G.G. Brusselle, T. Maes, et al., TNF alpha receptor genotype influences smoking-induced muscle-fibre-type shift and atrophy in mice, Acta Neuropathol. 115 (2008) 675–678, https://doi.org/10.1007/s00401-008-0348-4.

[18] N. Huang, M. Kny, F. Riediger, et al., Deletion of Nlrp3 protects from inflammation-induced skeletal muscle atrophy, Intensive. Care. Med. Exp. 5 (2017) 3, https://doi.org/10.1186/s40635-016-0115-0.

[19] J. Ding, B. Liu, P. Han, et al., Trichostatin A inhibits uterine histomorphology alterations induced by cigarette smoke exposure in mice, Life Sci. (2019), https://doi.org/10.1016/j.lfs.2019.04.069.

[20] C.S. Wu, Q. Wei, H. Wang, et al., Protective effects of ghrelin on fasting-induced muscle atrophy in aging mice, J. Gerontol. A Biol. Sci. Med. Sci. (2018), https://doi.org/10.1093/gerona/gly256.

[21] J.L. Brown, D.E. Lee, M.E. Rosa-Caldwell, et al., Protein imbalance in the development of skeletal muscle wasting in tumour-bearing mice, J. Cachexia. Sarcopenia Muscle 9 (2018) 987–1002, https://doi.org/10.1002/jcsm.12354.

[22] S. Yamaguchi, I. Fujii-Taira, A. Murakami, et al., Up-regulation of microtubule-associated protein 2 accompanying the filial imprinting of domestic chicks (Gallus gallus domesticus), Brain Res. Bull. 76 (2008) 282–288, https://doi.org/10.1016/j.brainresbull.2008.02.010.

[23] J. Ding, Y.F. Cong, B. Liu, et al., Aberrant protein turn-over associated with myofibrillar disorganization in FHL1 knockout mice, Front. Genet. 9 (2018) 273, https://doi.org/10.3389/fgene.2018.00273.

[24] J. Ding, Z. Peng, D. Wu, et al., A transcriptomics study of differentiated C2C12 myoblasts identified novel functional responses to 17beta-estradiol, Cell Biol. Int. 42 (2018) 965–974, https://doi.org/10.1002/cbin.10962.

[25] A.E.M. Kneppers, R.A.M. Haast, R.C.J. Langen, et al., Distinct skeletal muscle molecular responses to pulmonary rehabilitation in chronic obstructive pulmonary disease: a cluster analysis, J. Cachexia. Sarcopenia Muscle 10 (2019) 311–322, https://doi.org/10.1002/jcsm.12370.

[26] T. Ogasawara, S. Marui, E. Miura, et al., Effect of eicosapentaenoic acid on prevention of lean body mass depletion in patients with exacerbation of chronic obstructive pulmonary disease: a prospective randomized controlled trial, Clin. Nutr. ESPEN. 28 (2018) 67–73, https://doi.org/10.1016/j.clnesp.2018.09.076.

[27] E.M. Castillo, D. Goodman-Gruen, D. Kritz-Silverstein, et al., Sarcopenia in elderly men and women, The Rancho Bernardo Study, Am. J. Prev. Med 25 (2003) 226–231, https://doi.org/10.1016/S0749-3797(03)00197-1.

[28] P. Szulc, F. Duboeuf, F. Marchand, et al., Hormonal and lifestyle determinants of appendicular skeletal muscle mass in men: the MINOS study, Am. J. Clin. Nutr. 80 (2004) 496–503, https://doi.org/10.1093/ajcn/80.2.496.

[29] J.S. Lee, T.W. Auyeung, T. Kwok, et al., Associated factors and health impact of sarcopenia in older Chinese men and women: a cross-sectional study, Gerontology 53 (2007) 404–410, https://doi.org/10.1159/000107355.

[30] K. Kruger, G. Dischereit, M. Seimetz, et al., Time course of cigarette smoke-induced changes of systemic inflammation and muscle structure, Am. J. Physiol. Lung. Cell. Mol. Physiol. 309 (2015) L119–L128, https://doi.org/10.1152/ajplung.00074.2015.

[31] M. To, E.B. Swallow, K. Akashi, et al., Reduced HDAC2 in skeletal muscle of COPD patients, Respir. Res. 18 (2017) 99, https://doi.org/10.1186/s12931-017-0588-8.

[32] F. Ratti, F. Ramond, V. Moncollin, et al., Histone deacetylase 6 is a FoxO transcription factor-dependent effector in skeletal muscle atrophy, J. Biol. Chem. 290 (2015) 4215–4224, https://doi.org/10.1074/jbc.M114.600916.

[33] N. Hu, L. Yang, M. Dong, et al., Deficiency in adiponectin exaggerates cigarette smoking exposure-induced cardiac contractile dysfunction: role of autophagy, Pharmacol. Res. 100 (2015) 175–189, https://doi.org/10.1016/j.phrs.2015.08.005.

[34] W.J. Ting, J.J. Yang, C.H. Kuo, et al., Environmental tobacco smoke increases autophagic effects but decreases longevity associated with Sirt-1 protein expression in young C57BL mice hearts, Oncotarget 7 (2016) 39017–39025 https://doi.org/10.18632/oncotarget.9176.

[35] B. Jiang, Y. Guan, H.J. Shen, et al., Akt/PKB signaling regulates cigarette smoke-induced pulmonary epithelial-mesenchymal transition, Lung Cancer 122 (2018) 44–53 https://doi.org/10.1016/j.lungcan.2018.05.019.

[36] J.P. White, S. Gao, M.J. Puppa, et al., Testosterone regulation of Akt/mTORC1/FoxO3a signaling in skeletal muscle, Mol. Cell. Endocrinol. 365 (2013) 174–186 https://doi.org/10.1016/j.mce.2012.10.019.

[37] M. Yamamoto, N.P. Legendre, A.A. Biswas, et al., Loss of MyoD and Myf5 in skeletal muscle stem cells results in altered Myogenic programming and failed regeneration, Stem. Cell. Reports. 10 (2018) 956–969 https://doi.org/10.1016/j.stemcr.2018.01.027.

[38] F. Baruffaldi, D. Montarras, V. Basile, et al., Dynamic phosphorylation of the Myocyte enhancer factor 2Calpha1 splice variant promotes skeletal muscle regeneration and hypertrophy, Stem Cells 35 (2017) 725–738, https://doi.org/10.1002/stem.2495.

[39] S.N. Pandey, J. Cabotage, R. Shi, et al., Conditional over-expression of PITX1 causes skeletal muscle dystrophy in mice, Biol. Open. 1 (2012) 629–639, https://doi.org/10.1242/bio.20121305.

[40] X. Kong, L. Ma, E. Chen, et al., Identification of the regulatory elements and target genes of Megakaryopoietic transcription factor MEF2C, Thromb. Haemost. 119 (2019) 716–725, https://doi.org/10.1055/s-0039-1678694.

[41] A. Mal, M. Sturniolo, R.L. Schiltz, et al., A role for histone deacetylase HDAC1 in modulating the transcriptional activity of MyoD: inhibition of the myogenic program, EMBO J. 20 (2001) 1739–1753, https://doi.org/10.1093/emboj/20.7.1739.

[42] K. Ha, J.G. Buchan, D.M. Alvarado, et al., MYBPC1 mutations impair skeletal muscle function in zebrafish models of arthrogryposis, Hum. Mol. Genet. 22 (2013) 4967–4977, https://doi.org/10.1093/hmg/ddt344.

[43] Q. Zhou, P.H. Chu, C. Huang, et al., Ablation of Cypher, a PDZ-LIM domain Z-line protein, causes a severe form of congenital myopathy, J. Cell Biol. 155 (2001) 605–612, https://doi.org/10.1083/jcb.200107092.

[44] A. Vihola, L.L. Bachinski, M. Sirito, et al., Differences in aberrant expression and splicing of sarcomeric proteins in the myotonic dystrophies DM1 and DM2, Acta Neuropathol. 119 (2010) 465–479, https://doi.org/10.1007/s00401-010-0637-6.

[45] R. Al-Khalidi, C. Panicucci, P. Cox, et al., Zidovudine ameliorates pathology in the mouse model of Duchenne muscular dystrophy via P2RX7 purinoceptor antagonism, Acta. Neuropathol. Commun. 6 (2018) 27, https://doi.org/10.1186/s40478-018-0530-4.

[46] Q.L. Zhang, W. Wang, Y. Jiang, et al., GRGM-13 comprising 13 plant and animal products, inhibited oxidative stress induced apoptosis in retinal ganglion cells by inhibiting P2RX7/p38 MAPK signaling pathway, Biomed. Pharmacother. 101 (2018) 494–500, https://doi.org/10.1016/j.biopha.2018.02.107.

[47] G. Lee, J.Y. Lim, W.R. Frontera, Apoptosis in young and old denervated rat skeletal muscle, Muscle Nerve 55 (2017) 262–269, https://doi.org/10.1002/mus.25221.

[48] M. Wang, Y. Zhang, M. Xu, et al., Roles of TRPA1 and TRPV1 in cigarette smoke-induced airway epithelial cell injury model, Free Radic. Biol. Med. 134 (2019) 229–238, https://doi.org/10.1016/j.freeradbiomed.2019.01.004.